Predicting Abiotic TCE Transformation Rate Constants—A Bayesian Hierarchical Approach

Störiko, Anna; Valocchi, Albert J.; Werth, Charles; Schaefer, Charles E.

DOI
10.1111/gwmr.12667

Publication date
2024

Document Version
Final published version

Published in
Groundwater Monitoring & Remediation

Citation (APA)
Störiko, A., Valocchi, A. J., Werth, C., & Schaefer, C. E. (2024). Predicting Abiotic TCE Transformation Rate Constants—A Bayesian Hierarchical Approach. *Groundwater Monitoring & Remediation*, *44*(4), 67-79. https://doi.org/10.1111/gwmr.12667

Groundwater Monitoring&Remediation

Research Article

Predicting Abiotic TCE Transformation Rate Constants—A Bayesian Hierarchical Approach

by Anna Störiko, Albert J. Valocchi, Charles Werth and Charles E. Schaefer

Abstract

Fe(II) minerals can mediate the abiotic reduction of trichloroethylene (TCE), a widespread groundwater contaminant. If reaction rates are sufficiently fast for natural attenuation, the process holds potential for mitigating TCE pollution in groundwater. To assess the variability of abiotic TCE reduction rate constants, we collected pseudo-first-order rate constants for natural sediments and rocks from the literature, as well as intrinsic (surface-area-normalized) rate constants of individual minerals. Using a Bayesian hierarchical modeling approach, we were able to differentiate the contributions of natural variability and experimental error to the total variance. Applying the model, we also predicted rate constants at new sites, revealing a considerable uncertainty of several orders of magnitude. We investigated whether incorporating additional information about sediment composition could reduce this uncertainty. We tested two sets of predictors: reactive mineral content (measured by X-ray diffraction) combined with surface areas and intrinsic rate constants, or the extractable Fe(II) content. Knowledge of the mineral composition only marginally reduced the uncertainty of predicted rate constants. We attribute the low information gain to the inability to measure the (reactive) surface areas of individual minerals in sediments or rocks, which are subject to environmental factors like aqueous geochemistry and redox potential. In contrast, knowing the Fe(II) content reduced the uncertainty about the first-order rate constant by nearly two orders of magnitude, because the relationship between Fe(II) content and rate constants is approximately log–log-linear. We demonstrate how our approach provides estimates for the range of cleanup times for a simple example of diffusion-controlled transport in a contaminated aquitard.

Introduction

Trichloroethylene (TCE) is a widespread contaminant in groundwater aquifers worldwide (Bourg et al. 1992). It is present at many U.S. military bases and industrial sites because of its use—among others—as a degreasing agent and for dry-cleaning (Morrison and Murphy 2013; Hempel 2021). Over decades in groundwater aquifers, TCE has diffused into low-permeability zones. After source zone depletion, back-diffusion into aquifers often leads to concentrations that exceed the regulatory standard (You et al. 2020). The slow release of TCE from low-permeability zones makes remediation measures intricate and cost-intensive (O'Connor et al. 2018). Natural attenuation by biological and abiotic transformation processes is thus an attractive prospect, provided that degradation rates are sufficiently fast. In groundwater systems where the contaminant mass is mostly contained in diffusion-controlled rock matrices, even slow degradation (half-lives of 5 to 20 years) can strongly contribute to natural attenuation (Pierce et al. 2018).

Several degradation pathways of TCE are known. Most widely known is the microbial reductive dechlorination pathway, where microorganisms reduce TCE to dichloroethylene (DCE), vinyl chloride (VC), and eventually ethene under anaerobic conditions. This pathway is challenged, however, by the fact that toxic intermediate products, DCE and VC, often accumulate in groundwater due to slower kinetics or inhibition of the respective reaction steps. Additionally, the reaction depends on the presence of a functioning community of TCE degraders that possess the enzymes necessary to mediate the reaction, and suitable electron donors (Bradley 2003). Acidic conditions (pH below ~6) can also restrict degradation by microbial reductive dechlorination (Zhuang and Pavlostathis 1995; Steffan and Schaefer 2016).

Alternatively, TCE can be degraded abiotically through reactions mediated by ferrous minerals (He et al. 2015). The ferrous minerals serve as an electron donor that can reduce TCE to acetylene and possibly other reduced gases under anoxic conditions, or react with oxygen to produce hydroxyl radicals that oxidize TCE to organic acids under (micro-)oxic conditions. In controlled laboratory studies, acetylene is usually the primary reaction product observed under anaerobic conditions. Ethene and ethane, propane, and butane are also frequently observed and are believed to result from the hydrogenation of acetylene and

Article impact statement: A statistical analysis estimates uncertainty of first-order rate constants for anaerobic, abiotic reduction of trichloroethylene in sediments and rocks.

doi: 10.1111/gwmr.12643

coupling reactions at iron mineral surfaces (Arnold and Roberts 2000; Elsner et al. 2008; He et al. 2015; Schaefer et al. 2017). Under microoxic conditions, oxalic, glycolic, and glyoxylic acids have been observed (Pham et al. 2008; Schaefer et al. 2018). These products can be easily degraded by microorganisms, making abiotic degradation processes difficult to identify in the field. Several ferrous minerals have been shown to mediate the abiotic transformation of TCE, among them iron sulfides (pyrite, mackinawite), iron carbonates (siderite, ankerite), and iron-bearing clay minerals (Butler and Hayes 1999, 2001; Weerasooriya and Dharmasena 2001; Lee and Batchelor 2002a, 2002b; Jeong and Hayes 2007; Liang et al. 2007; He et al. 2010; Kim et al. 2013; Velimirovic et al. 2013; Schaefer et al. 2021).

In order to know if natural attenuation by abiotic transformation will mitigate TCE back diffusion, it is necessary to quantify rates of transformation at field sites. Pseudo-first-order rate constants are a common measure used to estimate how fast reactions occur. They are typically determined in batch experiments where TCE is incubated with sediments, and the concentrations of TCE and reaction products are monitored over time (e.g., Schaefer et al. 2018; Yin et al. 2023). They can also be determined in more complex settings, such as diffusion cell experiments in combination with a reactive transport model (Schaefer et al. 2013, 2015; Berns et al. 2019). However, experiments to determine rate constants are time-consuming and can only be done if a sample of the material is available. When an experimental determination of the rate constant is not a viable option for a particular site, rate constants can only be estimated by extrapolating from other sites, or possibly from site-specific information regarding ferrous minerals and their reactivity with TCE. In these cases, it is particularly important to consider the uncertainty of such a prediction.

Uncertainty about rate constants at new sites arises from several sources. The first source is physical variability between sites: sediments contain different amounts of reactive minerals, minerals vary in specific surface area, and the reactivity of a mineral normalized to its surface area may also vary between sediments, possibly due to differences in redox potential, amount of adsorbed ferrous iron, competing species undergoing reduction, organic matter coatings, etc. The second source is uncertainty about parameter values because measurements are imprecise. Finally, there is also uncertainty about the conceptual model and the "correct" mathematical description of reaction processes. For example, we may question if a first-order decay model is appropriate.

The goal of our study is to develop a statistical modeling approach to predict abiotic TCE reduction rate constants in natural sediments based on site-specific information regarding ferrous minerals and their reactivity with TCE that takes into account these uncertainties. Abiotic TCE oxidation rates may also be important (Damgaard et al. 2013; Berns et al. 2019), but are outside the scope of this effort. We will address the following specific questions:

- How large is the uncertainty of first-order rate constants of abiotic TCE reduction in natural sediments?
- How can we predict first-order rate constants for new sites based on the available ferrous mineral data?
- What types of additional information about a material are most helpful to reduce uncertainty of the rate constants?

We will not address the third source of uncertainty (conceptual uncertainty) quantitatively in this paper but will address how it affects estimates and predictions qualitatively.

To assess the variability of TCE reduction rate constants we have gathered values for a variety of materials that were available from the literature (He et al. 2010; Schaefer et al. 2015, 2017, 2018; Berns et al. 2019; Yu et al. 2020; Yin et al. 2023). We then unravel parameter uncertainty and physical variability of different materials using a Bayesian hierarchical modeling approach. Bayesian modeling is a statistical approach that provides a powerful and consistent way to handle uncertainty in observations, model parameters, and model structure. In the Bayesian framework, parameters are described by probability distributions instead of fixed values. These distributions express our degree of knowledge about the parameters. We can update our knowledge, and thus the distributions, by using information about parameters contained in observations, for example, measured rate constants determined in experiments. The hierarchical modeling approach, also called multilevel modeling, lets us account for physical variability between sediments by determining individual parameters for each sediment sample. However, we assume that each sediment sample is drawn from a common distribution of sediments with similar properties. By employing this approach, we can effectively predict the parameters and their associated uncertainty for sediments that have not yet been probed.

The range of measured pseudo-first-order rate constants for natural sediments is very broad when no additional information is taken into account. Measured half-lives range between less than 1 d to more than 1000 years. To reduce the predicted range of rate constants, we test two approaches of incorporating additional data about the material properties. First, we use information about the abundance of reactive minerals, and about the intrinsic rate constants of these minerals. Abiotic TCE reduction rate constants have also been determined for individual minerals (Butler and Hayes 1999, 2001; Weerasooriya and Dharmasena 2001; Lee and Batchelor 2002a, 2002b; Jeong and Hayes 2007; Liang et al. 2007; He et al. 2010; Kim et al. 2013; Velimirovic et al. 2013; Schaefer et al. 2021). We can integrate these data into the estimation of first-order rate constants if we assume that the overall first-order rate constant is composed of the contributions of individual minerals. Second, we consider the extractable Fe(II) content from dilute acid extraction as a predictive variable since it has shown a correlation with pseudo-first-order rate constants in earlier studies (Schaefer et al. 2013, 2018). Overall, we use three categories of data (tabulated in Tables S1 and S2 of the Supporting Information): (1) Pseudo-first-order rate constants of natural sediments, (2) intrinsic rate constants of pure minerals, and (3) data providing additional information about sediment composition (measured mineral mass fractions and extractable Fe(II) content).

We structure the remainder of the article as follows: First, we explain how to model first-order rate constants with a Bayesian hierarchical approach, accounting for experimental and parameter uncertainty and natural variability. We discuss how first-order rate constants of natural sediments can be linked to the reactive mineral and Fe(II) content of natural sediments. We illustrate how the results can be used to predict first-order rate constants at sites where TCE degradation has not previously been studied, either with known or with unknown sediment properties. Finally, we discuss what indicators or measurements are most suitable to reduce uncertainty of predicted TCE rate constants, based on our findings.

Methods

Accounting for Uncertainty and Variability with Bayesian Hierarchical Modeling

Bayesian Modeling and Parameter Inference

Bayesian modeling involves three main steps: model building, inference, and model checking or improvement (Gelman et al. 2020). First, we choose uncertain model parameters and a mathematical model that relates them to observed variables. Based on expert knowledge (e.g., physical constraints, literature values), we define *prior* probability distributions that represent reasonable ranges and our uncertainty about the parameters, without considering the data. Model building also encompasses defining a statistical model that describes our knowledge of how data are generated. In particular, we need to define the likelihood function, which represents the conditional probability of observing a given set of data, provided the parameters are known. The likelihood can also be interpreted as a measure of goodness-of-fit between the model and data.

In the inference step, prior distributions and likelihood are combined to obtain the updated *posterior* distribution. The posterior distribution usually needs to be approximated numerically, for example, using Markov chain Monte Carlo (MCMC) methods. This step is related to deterministic model calibration (e.g., maximum likelihood estimation), but it recovers samples from the full parameter distribution instead of a point estimate and thus provides an uncertainty estimate. Finally, we diagnose computational issues, assess convergence of the inference, evaluate model fit, compare alternative models, and make changes to prior distributions and the model structure in order to resolve problems.

Hierarchical Modeling of Sediment Variability

There are two sources of variability in measured first-order rate constants:

1. Physical variability between the sediments—for example, sediments can vary in their content of reactive minerals (we mean "physical" in the sense of "relating to material things"—that is, it can also relate to chemical properties).
2. Uncertainty arising because experimentally determined values are subject to measurement error. Replicate measurements or different experimental set-ups (e.g., batch vs. diffusion experiment, or differing aqueous geochemistry) yield different rate constants for the same sediment.

We can represent both of these sources of variability with probability distributions. The first distribution reflects how probable a certain rate constant is if we consider any kind of sediment, and we will call this the *global* parameter distribution. We specify this distribution for the *logarithm* of rate constants in order to take into account that natural variability ranges over several orders of magnitude. In addition, the log transformation ensures that estimated rate constants are positive. We assume that the log rate constants follow a normal distribution with mean $\mu_{\ln\Lambda}$ and standard deviation $\sigma_{\ln\Lambda}$, where $\sigma_{\ln\Lambda}$ represents the variability of rate constants caused by physical and chemical differences between natural sediments. The rate constant of any specific sediment j, $\ln(\lambda_j)$ is obtained from the global parameter distribution:

$$\ln(\lambda_j) \sim N(\mu_{\ln\Lambda}, {\sigma_{\ln\Lambda}}^2), \tag{1}$$

where $\sim$ means "follows the distribution of" (Figure 1). We can obtain information about the shape of the global distribution (that is, about $\mu_{\ln\Lambda}$ and $\sigma_{\ln\Lambda}$) by using data from several sediments. Rate constants from clayey sediments and rock matrices are assumed to originate from the same distribution. While a model that distinguishes the distributions of

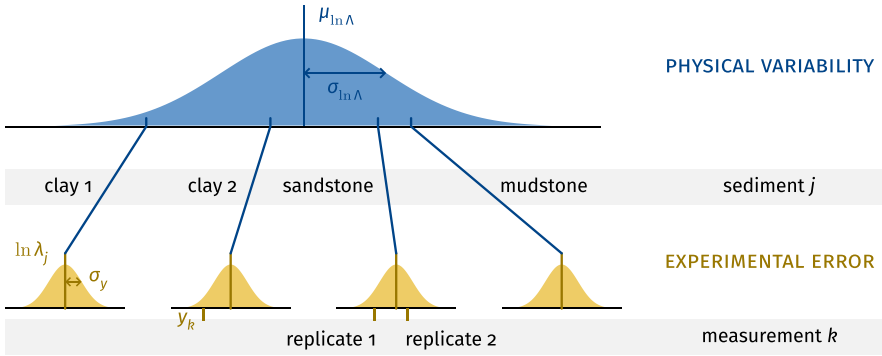

Figure 1. Sketch of the hierarchical model: The log rate constants of different sediments j follow a normal distribution (shown in blue) that represents physical variability. (The sketch examplarily shows only four sediments, not the full model and dataset.) Measurements follow a normal distribution representing experimental error around the log rate constants $\ln\lambda_j$ (shown in yellow). The parameters $\mu_{\ln\Lambda}$, $\sigma_{\ln\Lambda}$, and σ_y are uncertain, and therefore also described by probability distributions (not shown in the sketch).

these types of materials might be conceptually more appropriate, it would also require more data to infer the larger number of parameters.

We further assume that measured rate constants follow a normal distribution with standard deviation σ_y (representing experimental error) around λ_j on a log scale:

$$y_k \sim N\left(\ln\left(\lambda_{j_k}\right), {\sigma_y}^2\right), \tag{2}$$

where k is an index of the measurement, j_k is the sediment used in experiment k, and y_k is the log of the measured rate constant. The log transformation here means that we assume a relative error (expressed as a fraction or percentage) for the rate constants.

The parameters of those two distributions ($\mu_{\ln\Lambda}$, $\sigma_{\ln\Lambda}$, and σ_y) are not known, and we need to estimate them from the data. In a Bayesian context, we express our knowledge (or uncertainty) about parameters in terms of probability distributions. Thus, the parameters $\mu_{\ln\Lambda}$, $\sigma_{\ln\Lambda}$, and σ_y themselves are also assigned a distribution (the prior), that gets updated to a posterior distribution based on the data. Details about how we choose prior distributions can be found in Sections S2.1 and S2.2, Supporting Information, and Table S4.

Integrating Information about Mineral Composition and Fe(II) Content

Variability of rate constants in natural sediments is very large (Table S2), implying that rate constants for yet unobserved sediments are very uncertain. However, mineral reactivity is not completely random but can be linked to physical properties such as the presence of reactive minerals, or the total Fe(II) content. Accounting for this information in the prediction of rate constants could reduce uncertainty. A simple way to make more specific predictions would be to add another level to the statistical model that differentiates various sediment categories ("mudstone," "clay," "sandstone," etc.). That is, instead of using the same $\mu_{\ln\Lambda}$ and $\sigma_{\ln\Lambda}$ for all sediments, we could introduce one parameter per category. However, we do not follow this approach because the number of data points available for each category is too small. In addition, the variability of rate constants within each category could still be large because sediments from the same category may have very different amounts of reactive minerals. Instead, we consider two measures that have been considered previously to assess the potential of TCE degradation in natural sediments: the mass fraction of specific reactive minerals as determined by X-ray diffraction (XRD), and the Fe(II) content determined by extraction. We set up several models that link reactive mineral content or Fe(II) content to bulk first-order rate constants via empirical relationships, enabling us to leverage the information contained in the additional measurements.

Relating First-Order Rate Constants to Reactive Mineral Content

Several minerals that react with TCE can be present in a sediment at the same time. Similar to the approach taken by Yin et al. (2023), we assume that they do not directly interact with each other during TCE degradation, so that the reaction rates are simply additive. The reaction rate of TCE with one specific mineral is assumed to depend, apart from the TCE concentration, on

1. The amount of reactive mineral present,
2. The specific surface area of the mineral, and
3. Its intrinsic reactivity, which is encoded in the intrinsic, surface-area-normalized rate constant k_i (L/m^2/year).

Thus, we can relate theoretical first-order rate constant of sediment j, λ_j^* (1/year), to the intrinsic rate constants, specific reactive surface areas A_i (m^2/g) and mineral content ϕ_{ij} (g/g of solids) of the reactive minerals i, and the solid-to-liquid ratio w_j (g/L) of the sediment as follows:

$$\lambda_j^* = \sum_i k_i A_{ij} \phi_{ij} w_j, \tag{3}$$

where the index i represents the reactive minerals in the sediment, and j indexes the sediment. The asterisk superscript (*) is used to indicate that this is the *theoretically expected* rate constant based on the intrinsic rate constants of individual minerals, which we distinguish from the actual first-order rate constants λ_j, as further explained in Section 2.2.2. Note that we allow the mineral content and specific surface area of each mineral to vary between different sediment samples. The specific surface area of a mineral depends, for example, on grain size and the degree of crystallinity, which can vary with location.

In our model, we only consider a subset of minerals for the sum in Equation 3. We assume that all the reactivity toward TCE can be attributed to mackinawite (FeS), pyrite, siderite, and illite. This is certainly a simplification of reality. However, given the limited data available, we deem it necessary to reduce the complexity of the model and the number of parameters. Iron sulfide minerals tend to be much more reactive (on the order of several magnitudes) than other ferrous minerals with TCE. Therefore, they likely cause most of the reactivity when they are present. We chose siderite as an additional mineral even though its reactivity is comparable to other minerals because it was detected by XRD in several samples shown to be reactive toward TCE (Schaefer et al. 2018), and other carbonate minerals (ankerite, dolomite) are common in other samples with ferrous iron that show reactivity toward TCE (Schaefer et al. 2015; Berns et al. 2019). We note, however, that neither mackinawite, pyrite nor siderite is detected in many samples with reactivity toward TCE. This is likely due to the inability of XRD measurements to detect minerals that have a low abundance or are poorly crystalline.

In order to quantify the uncertainty of bulk rate constants, we treat the parameters k_i, A_{ij}, and ϕ_{ij} as random variables. That is, we do not use fixed values, but account for their uncertainty by using distributions of these parameters. For each mineral, we use the same k_i in all sediments. We specify a broad prior and then use measured intrinsic rate constants reported in the literature to update the distribution via the likelihood (Figure 2).

For the mineral contents ϕ_{ij}, we apply a hierarchical approach and estimate the mineral contents in each of the sediments as well as the parameters of a global distribution of mineral contents (details are provided in Section S2.2).

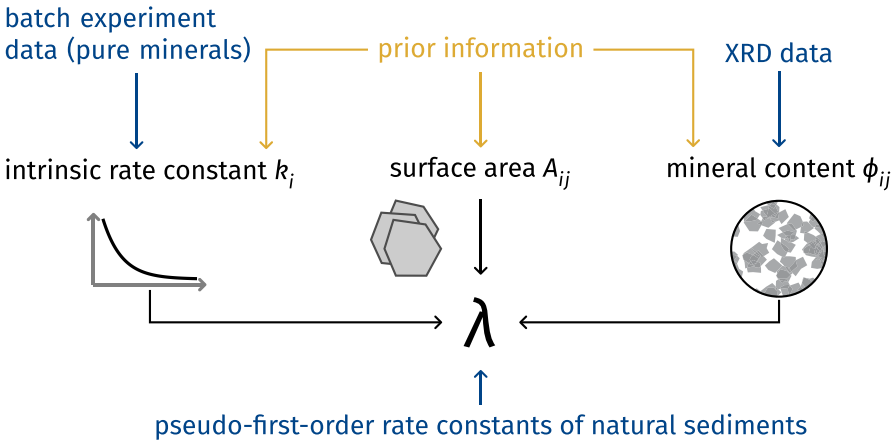

Figure 2. Conceptual model of the mineral content/surface area model, and data used to infer its parameters.

If XRD data are available for a sediment, we integrate the contained information about the mineral content into the model via the likelihood. We assume that data follow a censored normal distribution with constant standard deviation around the logit-transformed mineral content. This is a normal distribution that is truncated at the detection limit, with the probability mass below the detection limit added at the cutoff (see Section S2.3). We apply the logit transform—defined as $\text{logit}(x) = \ln\left(\frac{x}{1-x}\right)$—in order to map mineral fractions (ranging between 0 and 1) to the real numbers (Gelman 2014). For small values, it is similar to the log transform, so a constant error on the logit scale approximately corresponds to a relative error of the measured mineral content. Minerals with low abundance cannot be detected with XRD. However, a non-detection still provides information—namely that the mineral content is below the detection limit. In order to use this information, we set the mineral content of non-detected minerals to the detection limit (1%) and account for the censoring in the likelihood function (see Section S2.3). Because we adjust the likelihood function, the data points will provide information that the mineral content is *less than* 1% (and potentially much smaller), rather than *exactly* 1%.

We also use a hierarchical approach for the specific surface area A_{ij}. That is, we estimate the global distribution of surface areas of a mineral i, and the specific surface area of mineral i in each sediment j (details in Section S2.2). Because it is not possible to measure the surface area of individual minerals in natural sediments, the distributions of A_{ij} can be estimated only indirectly through measurements of the bulk TCE rate constants, intrinsic rate constants, and mineral contents.

The only parameter that we treat as fixed is the solid-to-liquid ratio w_j, because we consider its uncertainty to be small relative to that of other variables in the model. In order to simplify the model, we eliminated the parameter from the model by normalizing all rate constants by w_j. That is, we modified the likelihood given in Equation 2 as follows:

$$y_k \sim N\left(\ln\left(\lambda'_{j_k}\right), {\sigma_y}^2\right), \tag{4}$$

where $\lambda'_j = \frac{\lambda_j}{w_j}$ is the normalized rate constant.

Accounting for Reduced Reactivity of Natural Sediments

Based on our prior distributions of the intrinsic rate constants, specific surface areas and measured mineral contents, we computed the theoretical first-order rate constants of natural sediments in low permeability zones (using Equation 3). First-order rate constants of natural sediments reported in the literature vary over several orders of magnitude. However, all of them are smaller than the theoretically computed values obtained from rate constants of individual minerals (further details are provided in the results, Section 3.1.2.2). This lower effective reactivity of natural sediments can have various reasons. For example, not all the mineral surface area may be accessible for TCE because it may be blocked by sorbed compounds. Or, small-scale diffusion processes that are not resolved by the model limit the effective rate. We can account for the observed discrepancy between the theoretical and observed first-order rate constants of natural sediments by applying an empirical scaling factor q that reduces the intrinsic rate constants of individual minerals, making them less reactive. The so-called "corrected" parameter is denoted by λ_j:

$$\lambda_j = \sum_i q k_i A_{ij} \phi_{ij} w_j \tag{5}$$

We estimate the distribution of the parameter q alongside with other parameters through Bayesian inference. Even though q could depend on the sediment or mineral, we decide to use the same factor for all minerals and sediments given our limited amount of data.

Relating First-Order Rate Constants to Total Fe(II) Content

Several studies have shown a relationship between Fe(II) content of natural sediments or rocks and pseudo-first-order TCE reduction constants (Schaefer et al. 2013, 2018). Even though the materials differed widely in terms of the amounts and types of minerals present, the relationship between the Fe(II) and bulk reaction rates was approximately linear, when plotted on a log–log scale. Based on the results of these studies, we propose the following Bayesian regression model to predict rate constants from the Fe(II) content:

$$\ln\left(\lambda_j\right) = a \ln[\text{Fe(II)}]_j + b + \varepsilon_j \tag{6}$$

Here, a and b are the coefficients of the linear regression. A linear relation on the log–log scale corresponds to a power law on the non-log scale. This also means that at zero iron content, the TCE reduction rate constant is always zero. To account for the fact that the relationship is not perfectly linear but somewhat noisy, we add a stochastic error term $\varepsilon_j \sim N(0, \sigma_\varepsilon)$. This means that the first-order rate constant for each sediment may deviate a bit from the linear relationship. The parameters a, b, and σ_ε are estimated from the data, and their prior distributions are given in Table S4. Measured log rate constants are assumed to follow a normal distribution around the regressed rate constants $\ln(\lambda_j)$, with a measurement error σ_y (same as in Equation 2). In principle, the model error and measurement error could also be combined into a single error term. The advantage of separating both terms is that it allows us to get a more accurate uncertainty estimate for the rate constants predicted for new sediments.

In contrast to standard linear regression, we do not assume the explanatory variable (the logarithm of the Fe(II) content) to be known exactly. Instead, we suppose that $\ln[\mathrm{Fe(II)}]_j$ is unknown, and needs to be estimated from measurements z_k. To estimate the Fe(II) content in the sediments we once more take a hierarchical approach. The ln Fe(II) content of sediment j is assumed to follow

$$\ln[\mathrm{Fe(II)}]_j \sim N\left(\mu_{\ln[\mathrm{Fe(II)}]}, {\sigma_{\ln[\mathrm{Fe(II)}]}}^2\right), \tag{7}$$

where $\mu_{\ln[\mathrm{Fe(II)}]}$ and $\sigma_{\ln[\mathrm{Fe(II)}]}$ are the mean and standard deviation of the global ln[Fe(II)] distribution. We estimate $\mu_{\ln[\mathrm{Fe(II)}]}$ and $\sigma_{\ln[\mathrm{Fe(II)}]}$ through Bayesian inference from the data. For the data in experiment k we assume that

$$z_k \sim N\left(\ln[\mathrm{Fe(II)}]_{j_k}, \sigma_z\right), \tag{8}$$

where σ_z is the measurement error. Since replicate Fe(II) measurements are not available, it is not possible to estimate σ_z. Thus, we set it to a fixed value of 0.2, corresponding to a relative error of the Fe(II) content of about 22%.

Predictions of Rate Constants in New Sediments

After obtaining posterior distributions of all model parameters, we can predict the probability distribution of rate constants in sediments at sites where no measurements are available. Without additional information about a sediment (mineral content or Fe(II) content), this distribution is given by the "global" distribution of λ with parameters $\mu_{\ln\Lambda}$ and $\sigma_{\ln\Lambda}$. However, we can also compute predictive distributions that are conditional on a measured Fe(II) content or measured mineral contents.

Since the mineral contents cannot be determined exactly, we account for a measurement error as follows: instead of using fixed values of the mineral composition, we generate samples from a normal distribution around the logit-transformed value of the assumed measurement, using a fixed standard deviation. Since the logit transform is similar to the log-transform for small mineral contents, this approach is closely related to using a relative error of the mineral contents. We choose the standard deviation such that the corresponding relative error is about 10%. Similarly, we assume that the ln Fe(II) content follows a normal distribution with standard deviation 0.2 around the measured value to account for a relative measurement error of about 20%.

The predictive distributions represent the variability due to physical differences between sediments, parameter uncertainty, and uncertainty due to measurement errors in mineral content or Fe(II) content measurements. They do not include variance produced by experimental error in experiments to determine rate constants (parameterized by σ_y). We do not account for these errors in predictions because we are interested in what the actual rate constants of natural sediments are, not what rate constants could be observed in experiments.

Implementation

In total, we set up three models to estimate first-order rate constants of natural sediments and relate them to other sediment properties. An overview of the models is given in Table 1. We implement the models using the Python library PyMC (Salvatier et al. 2016; Wiecki et al. 2023) that enables a flexible and easy model specification. To sample the posterior distribution we use PyMC's default No-U-Turn (NUTS) sampler (Hoffman and Gelman 2014). It is designed to efficiently sample the parameter space by exploiting gradient information that is obtained through automatic differentiation. To assess convergence of the sampler, we run multiple independent MCMC chains and compute the rank-based diagnostic criterion $\widehat{R}$ (Vehtari et al. 2021) as implemented in the software package ArviZ (Kumar et al. 2019) (computed values are provided in Tables S4 to S6). Additionally, we compute the effective sample size and visually inspect trace plots, that is, graphs of the sampled parameter values plotted against the posterior draw. The Python code and data associated this study are openly available as a research compendium (Störiko et al. 2023).

Table 1

Overview of the Different Models Used

	Model Name	Additional Data Used	Equation
1	Only rate constants	None	None
2	Mineral content/surface area	Mineral content data (XRD), surface-area-normalized specific rate constants	$\lambda_j' = q \sum k_i A_{ij} \phi_{ij}$
3	Fe content	Fe(II) content data (acid extraction)	$\ln\left(\lambda_j'\right) = a\ln[\mathrm{Fe(II)}]_j + b + \varepsilon_j$

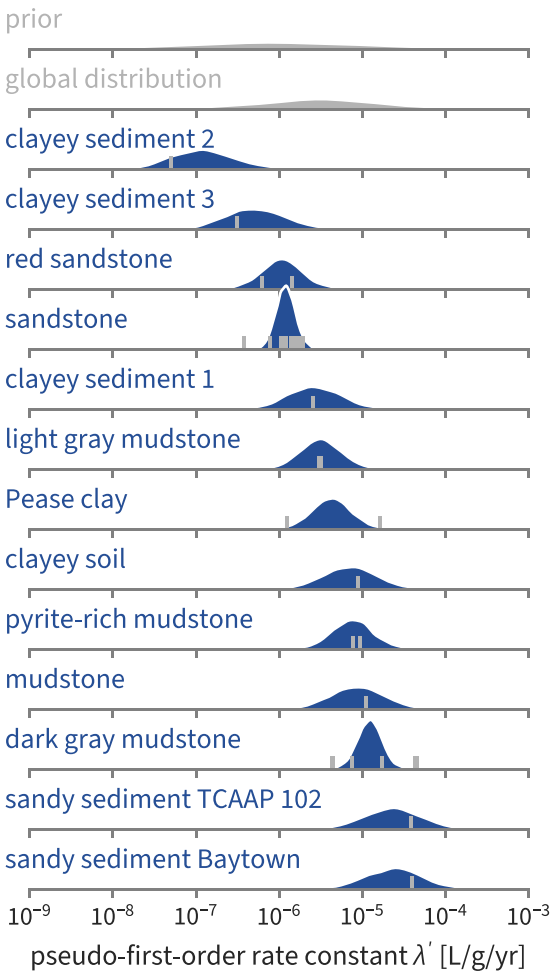

Figure 3. Distributions of pseudo-first-order rate constants in model 1 (only rate constants). The blue distributions show the posterior for rate constants of individual sediments λ_j. The gray distributions show the prior (same for all sediments) and the posterior of the global distribution. Data points are plotted as gray bars at the bottom of the axes. Note that some data points lie close to each other, making the bars appear wider.

Results and Discussion

Rate Constants of Natural Sediments and Rocks

Distribution Based on First-Order Rate Constant Data Only

Figure 3 shows pseudo-first-order rate constant data for different natural sediments that we collected from the literature (given in Table S2) as gray bars. Alongside, it shows the posterior distributions for the rate constants of each of the natural sediments (blue distributions) obtained with the *only rate constants* model. (The same plot is provided for the other models in Figures S3 and S4. Summary statistics of the posterior distributions of all model parameters are provided in Tables S5 to S7.) Even though the prior distribution (top of Figure 3) is the same for all sediments, the posterior distributions are different, because different data were used to update the distribution in each sediment.

The posteriors are considerably shifted compared to the prior, so that the distributions overlap with measured rate constants. In addition, the posterior distributions are narrower than the prior distribution. This shows that the posterior is strongly informed by the data. However, the effect of the data is not equally strong in all sediments. Distributions of sediments where several measurements are available (e.g., the *dark gray mudstone*) tend to be narrower than those where we could use only a single data point. One example of the latter is the *clayey sediment 2*: The posterior distribution of its rate constant is not centered around the measurement, but the mode sits somewhere in between the measurement and the mode of the global distribution. This shows the regularizing effect that the global distribution has when only little data are available.

The global distribution of rate constants (shown in gray) is broader than the distribution of any individual sediment because it takes into account the physical variability of natural sediments. It represents the range of reasonable rate constants for natural sediments in general and, thus, the range of values we need to consider when no measurements are available. Even though it is more narrow than the prior distribution, it still ranges over several orders of magnitude.

The lower tail of the global distribution extends to values as low as 10^{-8} L/g/year, which corresponds to a half-life of more than 1000 years, assuming a solid-to-liquid ratio of 6000 g/L. It is difficult to evaluate these small rate constants experimentally because time constraints and the accuracy of concentration measurements provide a lower limit to rate constant measurements. However, it is unclear exactly where such a limit would be, and it will be highly dependent on the experimental setup. Thus, the extent to which the distribution extends to small values will depend a lot on the prior distribution. In practice, however, it may not be so important how far the distribution extends at the low end. From a practitioner's point of view, these rate constants could all be considered to be zero, since they exclude the potential for site management by natural attenuation.

Rate Constants Predicted from the Contributions of Individual Minerals

Intrinsic rate constants of pure minerals. Figure 4A shows the surface-area normalized intrinsic rate constants (k_i) of several minerals that we collected from the literature (Table S3). For the minerals represented in our model, we also estimated posterior distributions of these rate constants based on the data (Figure 4B and Table S6). Posterior distributions of illite and siderite are only slightly shifted toward smaller values but are still broad, since little data are available to constrain them. In contrast, posterior distributions of pyrite and FeS are considerably narrower than the priors. Nevertheless, the uncertainty of surface-area-normalized rate constants of the individual minerals is large in the posterior distribution. This large uncertainty is caused by the wide spread of measured surface-area-normalized rate constants. The measured rate constants of pyrite and FeS range over six orders of magnitude (Figure 4). This is much larger than we could reasonably expect for variance produced by measurement errors. The large spread of the rate constants instead suggests that the experiments cannot measure *intrinsic* properties of the minerals, but that the obtained values depend on external factors that vary between the experiments.

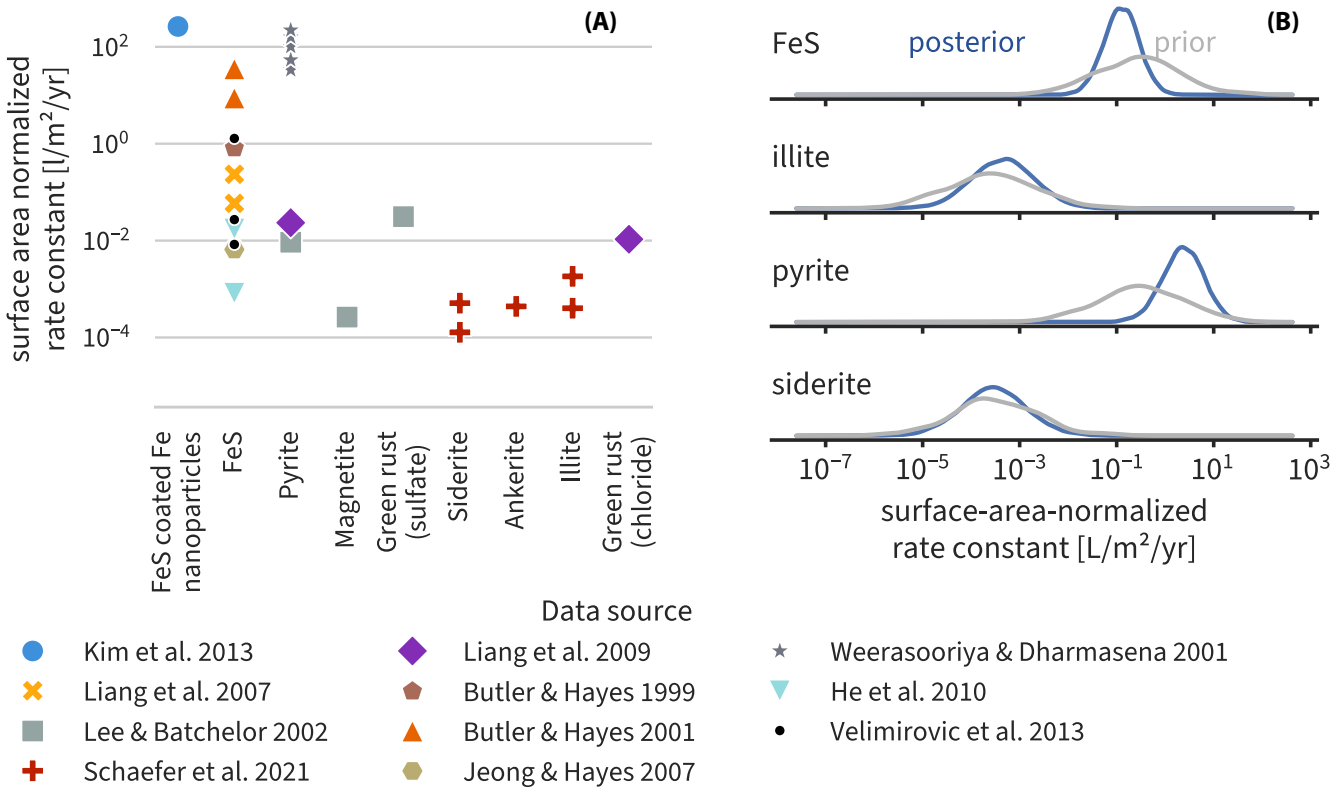

Figure 4. Intrinsic rate constants of anaerobic TCE reduction for different minerals. (A) Data gathered from the literature. (B) Kernel density estimates of the prior and posterior distributions.

One reason why the surface-area-normalized rate constants vary so widely is probably that the measured specific surface areas used for normalization (usually determined with N_2-BET) may not be representative of *reactive* surface areas. The normalization by reactive surface areas then adds noise to the rate constant data, *causing* part of the variance. Indeed, measured (log) rate constants for FeS and pyrite normalized to mass rather than surface area (i.e., L/g/d versus L/m²/d) exhibit a lower variance (see Figure S1).

Geochemical conditions also affect TCE reaction rates, potentially by modifying the reactive surface area. Several studies have reported that TCE transformation rate constants for iron sulfide minerals increase with pH (Butler and Hayes 2001; Weerasooriya and Dharmasena 2001). This effect has been attributed to the increasing deprotonation of surface groups with increasing pH, making the mineral more reactive. In addition, other water chemistry parameters (ionic composition, organic matter) are known to influence abiotic TCE transformation rate constants (Kim et al. 2013).

Another confounding factor could be that the assumed linear dependence on surface area does not reflect the actual reaction kinetics. A linear dependence on surface area is often assumed for reactions at the mineral–water interface if the rate is limited by the interfacial reaction (Brantley 2008). However, the exact reaction mechanism of abiotic TCE reduction at the surface of ferrous iron minerals is not known. Electron transfer at the surface of minerals with semiconducting properties—such as iron sulfides—can be fed by electron flow within the crystal (Yanina and Rosso 2008). This could potentially result in an overall rate law that does not depend linearly on mineral surface area.

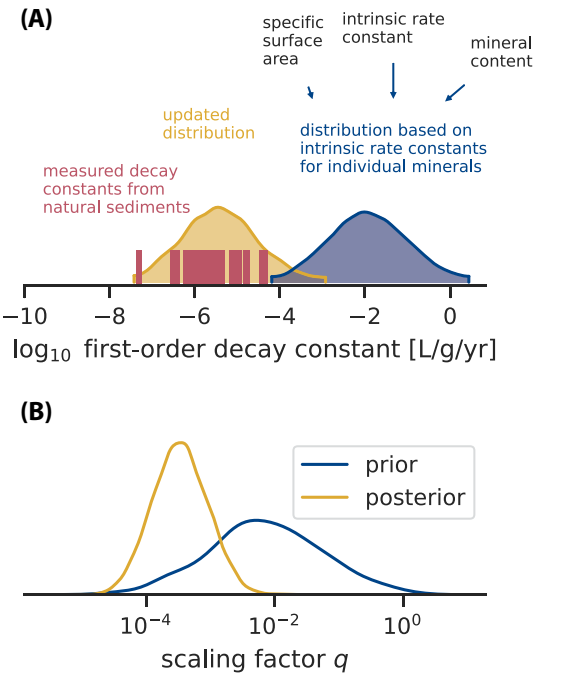

Figure 5. (A) Posterior distributions of theoretical rate constants based on intrinsic rate constants (Equation 3) of individual minerals and rate constants "corrected" based on observations. (B) Prior and posterior distribution of the scaling factor *q*.

Reduced reactivity of natural sediments compared to pure minerals: Based on the mineral-specific, intrinsic rate constants shown in Figure 4, we computed first-order

rate constants without accounting for a correction factor (using Equation 3). The mineral contents and surface areas were based on the respective global posterior distributions, reflecting the range that should be expected if no measurements are available. The resulting rate constants are much larger than observed rate constants of natural sediments (compare the blue distribution in Figure 5 to measurements indicated in red).

Only through the inclusion of the "correction" factor q (Equation 5) the posterior distribution of first-order rate constants is shifted to align with the measured values (yellow distribution in Figure 5). The posterior median of the correction factor q is 0.0003, showing that the natural sediments are several orders of magnitude less reactive than what we expected based on intrinsic rate constants, specific surface areas and typical mineral contents.

The importance of the scaling factor becomes evident if we calculate a rate constant solely based on literature values and expert knowledge, instead of using the Bayesian model that includes the scaling factor. We assume the following mineral composition: FeS: 0.01%, pyrite: 0.1%, siderite: 3%, illite: 10%, and surface areas: FeS: 140.00 m^2/g, pyrite: 0.01 m^2/g, siderite: 0.30 m^2/g, illite: 0.03 m^2/g. Using the mean of observed intrinsic rate constants (data in Figure 4A averaged on a log scale—FeS: 1.2×10^{-1} L/m^2/year, pyrite: 9.0 L/m^2/year, siderite: 2.6×10^{-4} L/m^2/year, illite: 8.6×10^{-4} L/m^2/year), we obtain a first-order rate constant for the sediment of 11 1/year. This is one order of magnitude larger than the *highest* measured rate constant (1.3 1/year).

Overall, the small scaling factor means that studies based on pure minerals cannot be easily extrapolated to natural sediments. Knowing the content of potentially reactive minerals in a sediment and the mineral-specific rate constants is not enough to predict the actual degradation potential.

This is a potential limitation of approaches that aim to determine the performance of abiotic degradation based on the presence of reactive minerals, such as the Min-Trap® sampler (Divine et al. 2023). Nevertheless, the Min-Trap® sampler is an intriguing approach because it examines the *formation* of new minerals rather than the mineral content of a sediment. These newly formed minerals could possibly be more reactive than existing Fe(II) minerals, contributing stronger to degradation. It will be interesting to see if the mineral contents from the sampler can indeed be predictive for rate constants of aquifer materials.

Rate Constants Predicted from Fe(II) Content

The logarithm of Fe(II) content and the logarithm of the pseudo-first-order rate constants are clearly positively related, and the relation can be approximated well by a log–log-linear relationship (Figure 6). Even though a relationship had been demonstrated earlier for individual datasets (Schaefer et al. 2013, 2018), our analysis shows that it also holds for our combined data set gathered from studies that used a variety of materials (sandstone, mudstones, clayey soils) and methods (batch experiments vs. diffusion–reaction experiments).

The posterior median of the slope parameter is 0.47, and the posterior median of the intercept is −16.4. Both parameters have considerable uncertainty in the posterior—the 5th and 95th percentile are [0.25, 0.68] and [−18.2, −14.4], respectively. The uncertainty of the slope parameter contributes to the predictive uncertainty of first-order rate constants. Adding more experimental data to the regression could reduce the uncertainty of the slope, and thus, the predictive uncertainty. The model error ϵ provides a measure of how much rate constants deviate from the linear relationship. Its posterior distribution ranges between 0.15 and 1.52 (5th and 95th percentile). These values provide an absolute

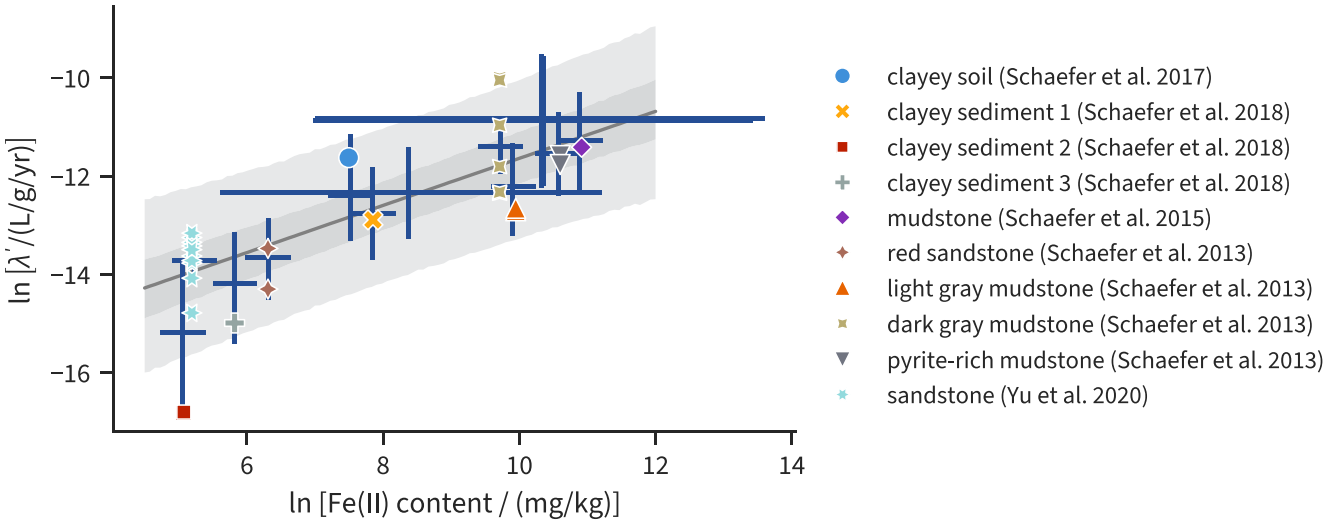

Figure 6. Modeled and observed relationship between Fe(II) content and pseudo-first-order rate constants. The gray line represents the posterior median of $\ln(\lambda')$. Gray shaded areas indicate the 90% and 50% highest density intervals of $\ln(\lambda')$. These intervals represent the total uncertainty of the regression, which is influenced by uncertainty of the regression parameters *a* and *b*, and by the error term ϵ_j. Blue crosses indicate posterior estimates of the Fe(II) content and rate constants for individual sediments. The intersection marks the median, and lines range between the 5th and 95th percentile of the posterior distribution. Colored markers indicate the measured values.

error on the log scale and can be converted to a relative error of the rate constants: the rate constants differ from the regression line by a factor between 1.16 and 4.59, that is, less than one order of magnitude. The posterior median of ϵ is 0.78, corresponding to a relative error of 2.18. Overall, this shows that the regression cannot be used to determine rate constants exactly, but it enables us to estimate the order of magnitude of the pseudo-first-order rate constants.

Predicting Rate Constants for New Sediments

We can predict rate constants at new sites where they have not been measured based on the posterior distributions of all three models. However, the predictions vary between the models. In the following, we assume that the solid-to-liquid ratio is known, and amounts to 6183 g/L, corresponding, for example, to a porosity of 30% and a bulk density of 1.85 kg/L.

If nothing is known about the site, the "global" distribution of λ provides an uncertainty estimate of the rate constant. Even though no measurement of the mineral content or Fe(II) content is available, this distribution can be computed based on the global distributions of mineral contents or Fe(II) content. The global rate constant distribution can be obtained with all three models, and the estimated posterior distributions are similar (even though the width of the distributions somewhat differs between models) because they are directly constrained by the same data. As discussed previously, the distribution is very broad because observed pseudo-first-order rate constants vary over several orders of magnitude (orange distributions in Figure 7, and gray distribution in Figure 3; the range from the 5th to the 95th percentile spans 2.7 orders of magnitude in the *only rate constants* model). That is, without further information about the composition of the material, the timescale of abiotic TCE degradation is essentially unknown.

We then computed the conditional distribution of the first-order rate constant λ, given that the mineral composition is known, for example by XRD measurements. Figure 7A shows the distribution of λ for a sediment containing 10% illite, 3% siderite, and just trace amounts of pyrite (0.1%) and mackinawite (0.01%). The information that we used is already more complete than what can be reasonably expected because XRD in general cannot detect minerals that are present at low contents (< 1 %). Predicting the first-order rate constants with the *mineral content/surface area* model, the uncertainty of λ for the sediment with known mineral composition is nearly as broad (2.6 orders of magnitude) as the distribution when no information is available about the mineral contents (3.1 orders of magnitude). However, it is slightly shifted toward smaller values, precluding the possibility of very large rate constants. Overall, the predictions suggest that knowing the mineral content provides only little information gain.

Alternatively, additional information about the sediment composition could be obtained from a measurement of the extractable Fe(II) content. We computed a posterior predictive distribution of λ conditional on a known Fe(II) content based on the regression model. As shown in Figure 7B, the posterior distribution for a sediment with known Fe(II) content is much narrower (1.4 orders of magnitude) than the distributions for sediment where either no additional information is available, or for the sediment with known mineral content shown in Figure 7A.

To illustrate how these rate constants translate into clean-up times at a contaminated site, we used a simple one-dimensional diffusion–reaction problem (for details, see Section S5). While our example is overly simplistic, rate constant estimates can also be combined with more elaborate site models to study the effect of degradation on attenuation of contaminant concentrations (Pierce et al. 2018). We assume that TCE is initially distributed uniformly in a relatively thin aquitard layer. Over time, it reacts inside the aquitard and diffuses out of the aquitard (see Figure S4). We neglect sorption of TCE onto the sediment. We computed the remaining mass as a fraction of the initial mass over time based on an analytical solution for diffusion in a sheet plane (Crank 1975, 48).

Assuming an aquifer thickness of 3 m, and an effective diffusion coefficient of 7.7×10^{-3} m^2/year (approximating tortuosity with a porosity of 0.3), the mass fraction remaining after 100 years assuming TCE is nonreactive is 67.0% (also see Figure S5). If we account for reactions (using the posterior of the global distribution), in contrast, the remaining mass ranges between 2×10^{-17}% and 61.3% (5th and 95th percentile), with a median of 10.0%. This shows that the abiotic TCE reduction has the potential to induce a considerably faster decrease of the contaminant mass in certain sediments, but has little effect in others. The uncertainty about the decrease in mass due to TCE reduction is very large. In the aquifer with a known Fe(II) content of 8000 mg/kg; however, the range of remaining mass is 2×10^{-6}% to

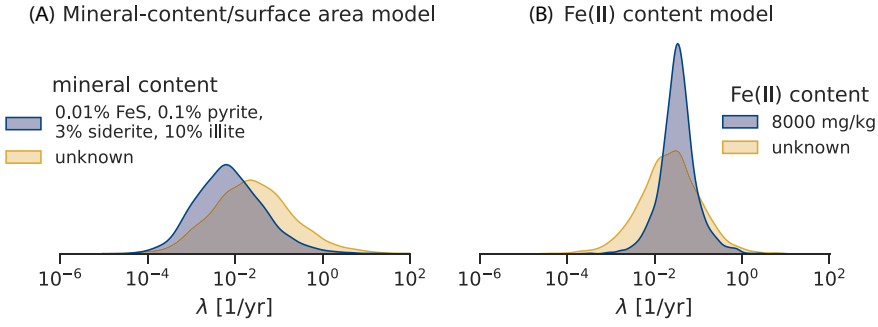

Figure 7. Comparison of the predicted first-order rate constants for a sediment with unknown properties compared to sediments with known mineral content (A) or known extractable Fe(II) content (B).

33.1% with a median of 2.3%. The prediction is much narrower, and in the considered scenario, it is very likely that the abiotic reduction reaction significantly decreases the TCE mass in the aquitard.

Implications for the Determination of TCE Reduction Potential

The data that we gathered in combination with our Bayesian hierarchical model show that abiotic TCE reduction rate constants in natural sediments and rocks range over several orders of magnitude. Physical variability between sediments is much larger than variance created through experimental error. This means that it is in general not possible to assess if abiotic reduction can make a substantial contribution to TCE degradation without additional information. Our findings suggest that both extractable Fe(II) content and mineral content information as obtained from XRD can provide such additional information and reduce uncertainty. However, extractable Fe(II) content leads to a stronger uncertainty reduction than mineral content data. It is thus a more helpful indicator to quantitatively predict the pseudo-first-order rate constants of natural rocks and sediments.

A possible explanation why Fe(II) content is a more powerful predictor is that it integrates several factors that importantly determine the reactivity of minerals, such as reactive surface area, or the fact that minerals do not always have exactly the same chemical composition. For example, the Fe(II) content of illite can vary with redox conditions. These differences would not be reflected in XRD data, but may be detectable in the extractable Fe(II) content. Mineral content information provides only relatively little quantitative information gain with respect to rate constants. To increase its benefit, we need a better understanding of the factors that cause variability of surface-area-normalized rate constants, and better measurements of reactive surface area. However, mineral content data can still be valuable to complement Fe(II) qualitatively because they can provide insight about the processes that create and maintain reactive minerals. For example, the presence of sulfide minerals indicates that microbial sulfate reduction is likely to be a contributing factor for sediment reactivity.

Another useful indicator of TCE reduction potential that we did not consider in this study could be measurements of the soil reduction–oxidation potential. Data from Schaefer et al. (2021) suggest that surface area normalized reaction rate constants of anaerobic, abiotic TCE reduction can be linearly related to the redox potential. Similarly, an empirical relationship between reduction potentials, pH and surface-area-normalized or mass-normalized rate constants could be shown for other contaminants (Stewart et al. 2018; Kocur et al. 2020). An empirical model that uses both redox potential measurements and extractable Fe(II) data can possibly further improve predictions of pseudo-first-order rate constants.

Even though additional information about the sediment composition can improve predictions of bulk reduction rate constants, the remaining uncertainty remains high with currently available data and models. Even when an Fe(II) content measurement is available, the uncertainty is about two orders of magnitude. Therefore, Fe(II) measurements alone do not provide sufficient evidence of abiotic degradation to adopt controlled natural attenuation as a remediation strategy. Rather, they can be used as a screening tool to assess whether there is sufficient potential to warrant more time-consuming and costly additional investigations, such as measurements of TCE abiotic reaction in batch vials using site sediment. Further, we need to consider that all measured rate constants used in this model were determined in lab experiments. In the field, factors and processes not present in small-scale experiments—for example, spatial heterogeneity of reactive minerals, or slow diffusion of TCE into reactive zones—could impact the effective TCE reduction rate. As the reduction of TCE oxidizes the reactive ferrous minerals, it can also lead to a decrease of the reactivity over time. In this case, the simple first-order rate law that our model is based on would not be appropriate. We thus expect that the overall uncertainty of reaction rates in the field is larger than the estimates obtained in this study.

Conclusions

We gathered a comprehensive set of experimentally determined rate constants of abiotic TCE degradation from available literature. The data reveal a large uncertainty both of pseudo-first-order rate constants in natural sediments and of intrinsic rate constants of pure minerals. Uncertainty about predicted rate constants in natural sediments could be reduced by complementary information about mineral composition or the extractable Fe(II) content, where the latter seems to be the better predictor. Integrating mineral content information required us to use a scaling factor that accounts for the fact that natural sediments were several orders of magnitude less reactive than expected from rate constants of pure minerals.

The high remaining predictive uncertainty (i.e., even when the mineral composition or Fe(II) content are known) underscores the importance of using modeling approaches that can provide uncertainty estimates, like Bayesian modeling. The uncertainty would have remained unnoticed with the standard linear regression approach used in the earlier analysis of subsets of the data (Schaefer et al. 2013, 2018). It also emphasizes the need to determine site-specific degradation constants in field or lab experiments when considering natural attenuation for contaminated site management.

The hierarchical Bayesian modeling approach provides a statistically rigorous framework to combine information and data from different types of experiments, or from different experimental conditions (Yu et al. 2015). In this study, it proved useful to differentiate several sources of variability present in the rate constant data set—showing that physical variability between sediments is larger than experimental error. The approach could also be applied in other cases where different levels of variability affect geochemical reaction rate constants. For example, we could use it to distinguish small-scale spatial heterogeneity from variability between sites, or to model variability of biogeochemical rate constants caused by differences in microbial community composition.

Acknowledgments

Support for this research was provided by the Strategic Environmental Research and Development Program (SERDP) under Project ER20-1203. Views, opinions, and/or findings contained in this report are those of the authors and should not be construed as an official Department of Defense position or decision unless so designated by other official documentation.

Data Availability Statement

This manuscript is accompanied by a research compendium that is openly available on Zenodo at 10.5281/zenodo.8399230. It contains the rate constant data collected from the literature, the Python code for data analysis and statistical modeling, the output data, and the notebooks for producing the manuscript.

Supporting Information

Additional Supporting Information may be found in the online version of this article. Supporting Information is generally not peer reviewed.

Data S1. Supporting Information.

References

Arnold, W.A., and A.L. Roberts. 2000. Pathways and kinetics of chlorinated ethylene and chlorinated acetylene reaction with Fe(0) particles. *Environmental Science & Technology* 34, no. 9: 1794–1805. https://doi.org/10.1021/es990884q

Berns, E.C., R.A. Sanford, A.J. Valocchi, T.J. Strathmann, C.E. Schaefer, and C.J. Werth. 2019. Contributions of biotic and abiotic pathways to anaerobic trichloroethene transformation in low permeability source zones. *Journal of Contaminant Hydrology* 224: 103480. https://doi.org/10.1016/j.jconhyd.2019.04.003

Bourg, A.C., C. Mouvet, and D.N. Lerner. 1992. A review of the attenuation of trichloroethylene in soils and aquifers. *Quarterly Journal of Engineering Geology and Hydrogeology* 25, no. 4: 359–370. https://doi.org/10.1144/GSL.QJEG.1992.025.04.10

Bradley, P.M. 2003. History and ecology of chloroethene biodegradation: A review. *Bioremediation Journal* 7, no. 2: 81–109. https://doi.org/10.1080/713607980

Brantley, S.L. 2008. Kinetics of mineral dissolution. In *Kinetics of Water-Rock Interaction*, ed. Susan L. Brantley, James D. Kubicki, and Art F. White, 151–210. New York: Springer.

Butler, E.C., and K.F. Hayes. 1999. Kinetics of the transformation of trichloroethylene and tetrachloroethylene by iron sulfide. *Environmental Science & Technology* 33, no. 12: 2021–2027. https://doi.org/10.1021/es9809455

Butler, E.C., and K.F. Hayes. 2001. Factors influencing rates and products in the transformation of trichloroethylene by iron sulfide and iron metal. *Environmental Science & Technology* 35, no. 19: 3884–3891. https://doi.org/10.1021/es010620f

Crank, J. 1975. *The Mathematics of Diffusion*, 2nd ed. Oxford: Clarendon Press.

Damgaard, I., P.L. Bjerg, J. Bælum, C. Scheutz, D. Hunkeler, C.S. Jacobsen, N. Tuxen, and M.M. Broholm. 2013. Identification of chlorinated solvents degradation zones in clay till by high resolution chemical, microbial and compound specific isotope analysis. *Journal of Contaminant Hydrology* 146: 37–50. https://doi.org/10.1016/j.jconhyd.2012.11.010

Divine, C., S. Justicia-León, J.M. Tilton, D. Liles, E. Carter, E. Zardouzian, K. Clark, D. Taggart, D. Freedman, S. LaRaia, F. Perrell, and K. Gerber. 2023. Min-Trap® samplers to passively monitor in-situ iron sulfide mineral formation for chlorinated solvent treatment. *Groundwater Monitoring & Remediation* 43, no. 3: 57–69. https://doi.org/10.1111/gwmr.12595

Elsner, M., M. Chartrand, N. VanStone, G.L. Couloume, and B.S. Lollar. 2008. Identifying abiotic chlorinated ethene degradation: Characteristic isotope patterns in reaction products with nanoscale zero-valent iron. *Environmental Science & Technology* 42, no. 16: 5963–5970. https://doi.org/10.1021/es8001986

Gelman, A. 2014. Bayesian Data Analysis. In *Chapman & Hall/CRC Texts in Statistical Science*, Third ed. Boca Raton, FL: CRC Press.

Gelman, A., A. Vehtari, D. Simpson, C.C. Margossian, B. Carpenter, Y. Yao, L. Kennedy, J. Gabry, P.-C. Bürkner, and M. Modrák. 2020. Bayesian workflow. *arXiv*. https://doi.org/10.48550/arXiv.2011.01808

He, Y.T., C. Su, J.T. Wilson, R.T. Wilkin, C.J. Adair, T.R. Lee, P. Bradley, and M. Ferrey. 2010. Identification and Characterization Methods for Reactive Minerals Responsible for Natural Attenuation of Chlorinated Organic Compounds in Ground Water. EPA/600/R-09/115. Washington, DC: U. S. Environmental Protection Agency.

He, Y.T., J.T. Wilson, S. Chunming, and R.T. Wilkin. 2015. Review of abiotic degradation of chlorinated solvents by reactive iron minerals in aquifers. *Groundwater Monitoring & Remediation* 35, no. 3: 57–75. https://doi.org/10.1111/gwmr.12111

Hempel, A. 2021. Trichloroethylene contamination of american military bases: An alternative toxic waste history. Undergraduate senior history thesis.

Hoffman, M.D., and A. Gelman. 2014. The No-U-Turn Sampler: Adaptively setting path lengths in Hamiltonian Monte Carlo. *Journal of Machine Learning Research* 15, no. 1: 1593–1623.

Jeong, H.Y., and K.F. Hayes. 2007. Reductive dechlorination of tetrachloroethylene and trichloroethylene by mackinawite (FeS) in the presence of metals: Reaction rates. *Environmental Science & Technology* 41, no. 18: 6390–6396. https://doi.org/10.1021/es0706394

Kim, E.-J., K. Murugesan, J.-H. Kim, P.G. Tratnyek, and Y.-S. Chang. 2013. Remediation of trichloroethylene by FeS-coated iron nanoparticles in simulated and real groundwater: Effects of water chemistry. *Industrial & Engineering Chemistry Research* 52, no. 27: 9343–9350. https://doi.org/10.1021/ie400165a

Kocur, C.M.D., D. Fan, P.G. Tratnyek, and R.L. Johnson. 2020. Predicting abiotic reduction rates using cryogenically collected soil cores and mediated reduction potential measurements. *Environmental Science & Technology Letters* 7, no. 1: 20–26. https://doi.org/10.1021/acs.estlett.9b00665

Kumar, R., C. Carroll, A. Hartikainen, and O. Martin. 2019. ArviZ a unified library for exploratory analysis of Bayesian models in Python. *Journal of Open Source Software* 4, no. 33: 1143. https://doi.org/10.21105/joss.01143

Lee, W., and B. Batchelor. 2002a. Abiotic reductive dechlorination of chlorinated ethylenes by iron-bearing soil minerals. 1. Pyrite and magnetite. *Environmental Science & Technology* 36, no. 23: 5147–5154. https://doi.org/10.1021/es025836b

Lee, W., and B. Batchelor. 2002b. Abiotic reductive dechlorination of chlorinated ethylenes by iron-bearing soil minerals. 2. Green rust. *Environmental Science & Technology* 36, no. 24: 5348–5354. https://doi.org/10.1021/es0258374

Liang, X., Y. Dong, T. Kuder, L.R. Krumholz, R. Paul Philp, and E.C. Butler. 2007. Distinguishing abiotic and biotic transformation of tetrachloroethylene and trichloroethylene by stable carbon isotope fractionation. *Environmental Science & Technology* 41, no. 20: 7094–7100. https://doi.org/10.1021/es070970n

Morrison, R.D., and B.L. Murphy. 2013. *Chlorinated Solvents: A Forensic Evaluation*. Cambridge: The Royal Society of Chemistry. https://doi.org/10.1039/9781849737265

O'Connor, D., D. Hou, Y.S. Ok, Y. Song, A.K. Sarmah, X. Li, and F.M.G. Tack. 2018. Sustainable in situ remediation of recalcitrant organic pollutants in groundwater with controlled release materials: A review. *Journal of Controlled Release* 283: 200–213. https://doi.org/10.1016/j.jconrel.2018.06.007

Pham, H.T., M. Kitsuneduka, J. Hara, K. Suto, and C. Inoue. 2008. Trichloroethylene transformation by natural mineral pyrite: The deciding role of oxygen. *Environmental Science & Technology* 42, no. 19: 7470–7475. https://doi.org/10.1021/es801310y

Pierce, A.A., S.W. Chapman, L.K. Zimmerman, J.C. Hurley, R. Aravena, J.A. Cherry, and B.L. Parker. 2018. DFN-M field characterization of sandstone for a process-based site conceptual model and numerical simulations of TCE transport with degradation. *Journal of Contaminant Hydrology* 212: 96–114. https://doi.org/10.1016/j.jconhyd.2018.03.001

Salvatier, J., T.V. Wiecki, and C. Fonnesbeck. 2016. Probabilistic programming in Python using PyMC3. *PeerJ Computer Science* 2: e55. https://doi.org/10.7717/peerj-cs.55

Schaefer, C.E., R.M. Towne, D.R. Lippincott, V. Lazouskaya, T.B. Fischer, M.E. Bishop, and H. Dong. 2013. Coupled diffusion and abiotic reaction of trichlorethene in minimally disturbed rock matrices. *Environmental Science & Technology* 47, no. 9: 4291–4298. https://doi.org/10.1021/es400457s

Schaefer, C.E., R.M. Towne, D.R. Lippincott, P.J. Lacombe, M.E. Bishop, and H. Dong. 2015. Abiotic dechlorination in rock matrices impacted by long-term exposure to TCE. *Chemosphere* 119: 744–749. https://doi.org/10.1016/j.chemosphere.2014.08.005

Schaefer, C.E., P. Ho, C. Gurr, E. Berns, and C. Werth. 2017. Abiotic dechlorination of chlorinated ethenes in natural clayey soils: Impacts of mineralogy and temperature. *Journal of Contaminant Hydrology* 206: 10–17. https://doi.org/10.1016/j.jconhyd.2017.09.007

Schaefer, C.E., P. Ho, E. Berns, and C. Werth. 2018. Mechanisms for abiotic dechlorination of trichloroethene by ferrous minerals under oxic and anoxic conditions in natural sediments. *Environmental Science & Technology* 52, no. 23: 13747–13755. https://doi.org/10.1021/acs.est.8b04108

Schaefer, C.E., P. Ho, E. Berns, and C. Werth. 2021. Abiotic dechlorination in the presence of ferrous minerals. *Journal of Contaminant Hydrology* 241: 103839. https://doi.org/10.1016/j.jconhyd.2021.103839

Steffan, R.J., and C.E. Schaefer. 2016. Current and future bioremediation applications: Bioremediation from a practical and regulatory perspective. In *Organohalide-Respiring Bacteria*, ed. Lorenz Adrian, and Frank E. Löffler, 517–540. Berlin, Heidelberg: Springer. https://doi.org/10.1007/978-3-662-49875-0_22

Stewart, S.M., T.B. Hofstetter, P. Joshi, and C.A. Gorski. 2018. Linking thermodynamics to pollutant reduction kinetics by Fe^{2+} bound to iron oxides. *Environmental Science & Technology* 52, no. 10: 5600–5609. https://doi.org/10.1021/acs.est.8b00481

Störiko, A., A.J. Valocchi, C. Werth, and C.E. Schaefer. 2023. Hierarky: Bayesian hierarchical modeling of abiotic TCE reduction rate constants. *Zenodo*. https://doi.org/10.5281/zenodo.8399230

Vehtari, A., A. Gelman, D. Simpson, B. Carpenter, and P.-C. Bürkner. 2021. Rank-normalization, folding, and localization: An improved $\hat{R}$ for assessing convergence of MCMC. *Bayesian Analysis* 16, no. 2: 667–718. https://doi.org/10.1214/20-BA1221

Velimirovic, M., P.-O. Larsson, Q. Simons, and L. Bastiaens. 2013. Reactivity screening of microscale zerovalent irons and iron sulfides towards different CAHs under standardized experimental conditions. *Journal of Hazardous Materials* 252–253: 204–212. https://doi.org/10.1016/j.jhazmat.2013.02.047

Weerasooriya, R., and B. Dharmasena. 2001. Pyrite-assisted degradation of trichloroethene (TCE). *Chemosphere* 42, no. 4: 389–396. https://doi.org/10.1016/S0045-6535(00)00160-0

Wiecki, T., J. Salvatier, R. Vieira, M. Kochurov, A. Patil, M. Osthege, B.T. Willard, B. Engels, C. Carroll, O.A. Martin, A. Seyboldt, A. Rochford, L. Paz, K. Meyer, P. Coyle, M.E. Gorelli, O. Abril-Pla, R. Kumar, J. Lao, V. Andreani, T. Yoshioka, G. Ho, T. Kluyver, K. Beauchamp, A. Andorra, D. Pananos, E. Spaak, B. Edwards, and E. Ma. 2023. Pymc-Devs/Pymc: V5.3.1. Zenodo. https://doi.org/10.5281/zenodo.7868623.

Yanina, S.V., and K.M. Rosso. 2008. Linked reactivity at mineral-water interfaces through bulk crystal conduction. *Science* 320, no. 5873: 218–222. https://doi.org/10.1126/science.1154833

Yin, X., H. Hua, J. Dyer, R. Landis, D. Fennell, and L. Axe. 2023. Degradation of chlorinated solvents with reactive iron minerals in subsurface sediments from redox transition zones. *Journal of Hazardous Materials* 445: 130470. https://doi.org/10.1016/j.jhazmat.2022.130470

You, X., S. Liu, C. Dai, Y. Guo, G. Zhong, and Y. Duan. 2020. Contaminant occurrence and migration between high- and low-permeability zones in groundwater systems: A review. *Science of the Total Environment* 743: 140703. https://doi.org/10.1016/j.scitotenv.2020.140703

Yu, Y., S. Steinschneider, and D.A. Reckhow. 2015. Evaluation of environmental degradation kinetics using hierarchical Bayesian modeling. *Journal of Environmental Engineering* 141, no. 12: 06015008. https://doi.org/10.1061/(ASCE)EE.1943-7870.0000997

Yu, R., L.C. Murdoch, R.W. Falta, R.G. Andrachek, A.A. Pierce, B.L. Parker, J.A. Cherry, and D.L. Freedman. 2020. Chlorinated ethene degradation rate coefficients simulated with intact sandstone core microcosms. *Environmental Science & Technology* 54, no. 24: 15829–15839. https://doi.org/10.1021/acs.est.0c05083

Zhuang, P., and S.G. Pavlostathis. 1995. Effect of temperature, pH and electron donor on the microbial reductive dechlorination of chloroalkenes. *Chemosphere* 31, no. 6: 3537–3548. https://doi.org/10.1016/0045-6535(95)00204-L

Biographical Sketches

Anna Störiko *is at Department of Water Management, Technische Universiteit Delft Faculteit Civiele Techniek en Geowetenschappen, Stevinweg 1, Delft 2600 GA, Netherlands; Department of Civil & Environmental Engineering, University of Illinois at Urbana-Champaign, 205 N. Mathews Avenue, Urbana, IL 61801.*

Albert J. Valocchi*, corresponding author, is at Department of Civil and Environmental Engineering, University of Illinois at Urbana-Champaign, 205 N. Mathews Street, Urbana, IL 61801; valocchi@illinois.edu*

Charles Werth *is at Department of Environmental and Water Resources Engineering, The University of Texas at Austin, Austin, TX.*

Charles E. Schaefer *is at CDM Smith, 110 Fieldcrest Avenue, #8 6th Floor, Edison, NJ 8837.*